Acta Med. Okayama, 2025
Vol. 79, No. 2, pp. 75–80

Acta Medica Okayama
http://escholarship.lib.okayama-u.ac.jp/amo/

Original Article

Potential for Radiation Dose Reduction in Temporal Bone CT Imaging Using Photon-Counting Detector CT

Fumiyo Higaki[a]*, Yusuke Morimitsu[b], Toshihiro Iguchi[c], Sung Il Hwang[d], Takahiro Kitayama[a], Yuka Takahashi[a], Mayu Uka[a], Noriaki Akagi[b], Akiko Sugaya[e], Toshiharu Mitsuhashi[f], Yusuke Matsui[g], and Takao Hiraki[g]

Departments of [a]Radiology, [b]Radiological Technology, [e]Otolaryngology-Head and Neck Surgery, [f]Center for Innovative Clinical Medicine, Okayama University Hospital, [c]Department of Radiological Technology, Faculty of Health Sciences, Okayama University, [g]Department of Radiology, Okayama University Faculty of Medicine, Dentistry and Pharmaceutical Sciences, Okayama 700-8558, Japan, [d]Department of Radiology, Seoul National University Bundang Hospital, Seongnam 13620, Korea

Temporal bone computed tomography (CT) is frequently performed for pediatric patients with ear diseases. Advances in CT technology have improved diagnostic imaging quality, but reduction of radiation exposure remains a goal. We evaluated the potential for radiation dose reduction in temporal bone CT examinations using porcine ear ossicles and a photon-counting detector CT system. Three scans of the bilateral temporal bone were performed on each of three pig cadaver heads. In each of seven successive imaging sessions, the radiation dose was reduced by an additional one-seventh of the recommended dose (RD). Two board-certified radiologists independently scored the resulting images on a scale of 1 to 5 points, where 5 represented the image quality at the RD. Images scoring ≥4.5 points were considered acceptable. Noise was assessed in a 2-cm-diameter region near the ear ossicles, and standard deviation was measured for each of the seven decrements from the RD. As the radiation dose decreased, the noise progressively increased, and visual assessment scores progressively decreased. Acceptable image scores were obtained at six-sevenths (4.9), five-sevenths (4.8), four-sevenths (4.7), and three-sevenths (4.6) of the RD. Thus, acceptable porcine temporal bone CT images were obtained with a radiation dose reduction of approximately 50%.

Key words: computed tomography, photon-counting detector computed tomography, ear ossicle, energy-integrating detector computed tomography

Computed tomography (CT) has become widely used and indispensable in daily clinical practice. Advances in CT technology have improved diagnostic imaging quality and provided many benefits to patients. However, CT has the unavoidable disadvantage of exposure to ionizing radiation, and there is considerable interest in further reducing patients' radiation exposure.

Temporal bone CT scans are performed for patients with a variety of ear diseases including congenital malformations of the ossicles, otitis media with osteoma, tympanosclerosis, and traumatic separation of the ossicles [1,2]. In these diseases, which often affect children, pre- and postoperative evaluations of the otoacoustic ossicles are important, and CT scans are thus performed aggressively. There is thus a serious need to realize lower radiation doses at the time of imaging.

Received July 1, 2024; accepted November 27, 2024.
*Corresponding author. Phone: +81-86-235-7313; Fax: +81-86-235-7316
E-mail: fumiyo.higaki@okayama-u.ac.jp (F. Higaki)

Conflict of Interest Disclosures: No potential conflict of interest relevant to this article was reported.

The recently developed photon-counting detector CT (PCD-CT) system uses a photon-counting detector (PCD) to measure the number of incident X-ray photons and their energy [3,4], rather than the energy-integrating detector (EID) used in the conventional CT system. The PCD-CT thus provides higher-resolution images with less image noise [5,6]. These images can be particularly useful for evaluating fine bone tissue such as that in the temporal bone area, including the ear ossicles [1,7]. PCD-CT may be more suitable for evaluating the ear ossicles than conventional CT models because it produces acceptable images at a lower radiation dose [5]. However, the efficacy of low-dose imaging of ear ossicles in clinical practice with this new CT technology has not yet been fully evaluated.

We conducted the present study to investigate the extent of radiation dose reduction that could be attained while obtaining diagnostic images in temporal bone CT examinations with PCD-CT. We used pig's ear ossicles as an ex vivo model, and the noise was not significantly increased.

Materials and Methods

Temporal bone CT images. Three pig cadaver heads for eating were purchased and used for CT imaging. The size of each cadaver pig head was approximately 280×200 mm. A total of nine CT scans of the bilateral temporal bone were performed three times per pig on separate days with a NAEOTOM Alpha PCD-CT system (Siemens Healthineers, Forchheim, Germany). The clinical imaging conditions were set as the recommended dose (RD) as detailed in Table 1.

At each successive imaging session, the radiation dose was reduced by an additional seventh of the RD to obtain CT images at seven different radiation doses (*i.e.*, the RD [as a reference], six-sevenths of the RD, five-sevenths of the RD, four-sevenths of the RD, three-sevenths of the RD, two-sevenths of the RD, and one-seventh of the RD) (Fig. 1).

Image analysis. Visual and noise assessments were performed on the obtained CT images. A total of

Table 1 Clinical imaging conditions (recommended dose)

Tube voltage	120 kV
Tube current	Quality ref. mAs 252
CTDI vol.	38.7～46.3 mGy (16 cm)
Collimation	120 × 0.2 mm-UHR mode
Rotation time	0.5 s
Pitch	0.55
Kernel	Hr 76.
Strength of iterative reconstruction	QIR 1
FOV	100 × 100 mm
Image matrix	512
Slice thickness	0.2 mm

CTDI, computed tomography dose index; UHR, ultra-high resolution; QIR, quantum iterative reconstruction; FOV, field of view.

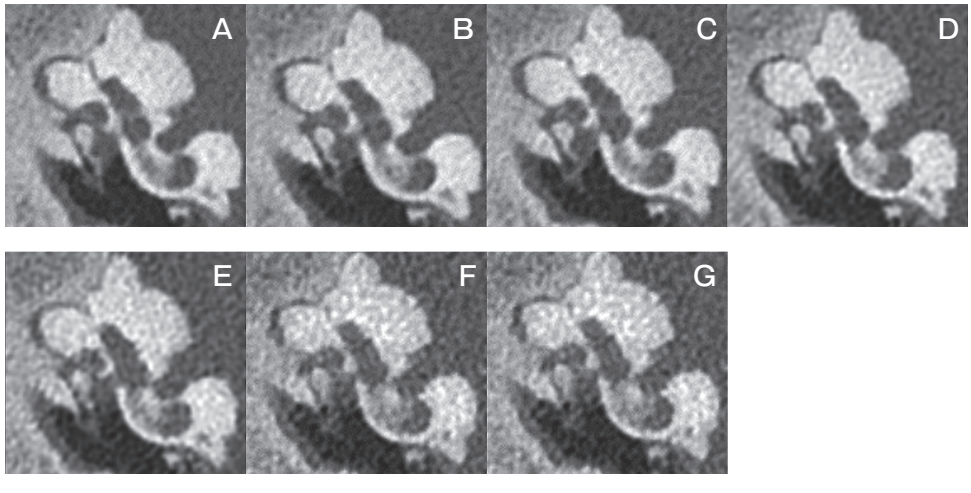

Fig. 1 CT images obtained with seven different radiation doses in the same porcine right-ear ossicle. The seven CT images were obtained at the recommended dose (RD) (**A**: 60 mGy), six-sevenths of the RD (**B**: 51 mGy), five-sevenths of the RD (**C**: 42 mGy), four-sevenths of the RD (**D**: 34 mGy), three-sevenths of the RD (**E**: 25 mGy), two-sevenths of the RD (**F**: 17 mGy) and one-seventh of the RD (**G**: 8 mGy).

18 bilateral ear ossicles (*i.e.*, 9 right and 9 left ossicles) were used for visual assessment. Two board-certified diagnostic radiologists from two different countries with 20 years (S.H.) and 10 years (T.K.) of experience independently scored the images as follows: 5 points (excellent score [*i.e.*, image at RD]), 4 points (good score), 3 points (possible score), 2 points (poor score), or 1 point (not diagnostic). Acceptable images were defined as those with a score ≥ 4.5 points.

For the noise assessment, a 2-cm-diameter region of interest was identified in the vicinity of the ear ossicles (Fig. 2), and the standard deviation was measured for each of the seven steps from the RD in a total of 18 bilateral ear ossicles (*i.e.*, 9 right and 9 left ossicles).

Statistical analysis. The scores of each of the six images (obtained using one-seventh to six-sevenths of the RD) were tested with a Wilcoxon matched-pairs signed-rank test for the difference in scores from the RD images. Because these were multiple tests, alpha was adjusted by the Holm method to control for family-wise error rates. The inter-rater agreement between the two raters was evaluated using weighted kappa statistics. The weights were $1-\{(i-j)/(k-1)\}^2$, where i and j index the rows and columns of the ratings by the two raters, and k is the maximum number of possible ratings. Since no images had a rating score of 1, we used $k=4$.

Alpha was set at 0.05, and p-values < 0.05 were considered significant. However, to keep the family-wise error rate within 5% in multiple tests, an alpha of 0.05 or less was used to determine the significance of individual test results. The statistical analyses were performed using Stata ver. 18 (Stata Corp., College Station, TX, USA) and Statistical Package for Social Science ver. 22.0 software (IBM, Armonk, NY, USA).

Fig. 2 The region of interest used for the noise assessment.

Results

As the radiation dose decreased, the image quality also decreased. The results of the visual assessment of each score are depicted in Figure 3. There was no significant difference between the scores of the images taken at the RD and the scores of the images obtained at six-seventh of the RD (mean score 4.9 points) ($p=0.125$). However, there was a significant difference between the scores of the images at the RD and those at ≤ five-sevenths of the RD; the images at five-sevenths, four-sevenths, and three-sevenths of the RD had mean scores of 4.8 ($p=0.0039$), 4.7 ($p=0.0005$), and 4.6 points ($p=0.0001$), respectively and were therefore considered acceptable images. The unacceptable CT images at two-sevenths and one-seventh of the RD had much lower scores at the means 4.1 ($p<0.0001$) and 3.1 ($p<0.0001$), respectively.

The average noise of the radiation dose reduction from the RD is illustrated in Fig. 4. The average noise value of the images at the RD was 161.5. The noise increased gradually as the radiation dose decreased, as follows: 171.7 (six-sevenths of the RD), 186.2 (five-sevenths of the RD), 201.2 (four-sevenths of the RD), 222.5 (three-sevenths of the RD), 250.7 (two-sevenths of the RD), and 287.9 (one-seventh of the RD). There were significant differences between the noise at the RD and the noise at ≤ six-sevenths of the RD; the noise at six-sevenths ($p=0.0002$), five-sevenths ($p<0.0001$), four-sevenths ($p<0.0001$), three-sevenths ($p<0.0001$), two-sevenths ($p<0.0001$), and one-seventh ($p<0.0001$) of the RD.

The expected agreement between raters was 88.02%, and the observed agreement was 95.41%. The weighted kappa statistics was thus 0.6171, and the inter-rater agreement was considered good.

Discussion

The results of this *ex vivo* study demonstrated an increase in noise and a decrease in visual assessment scores with decreasing radiation doses. For the visual

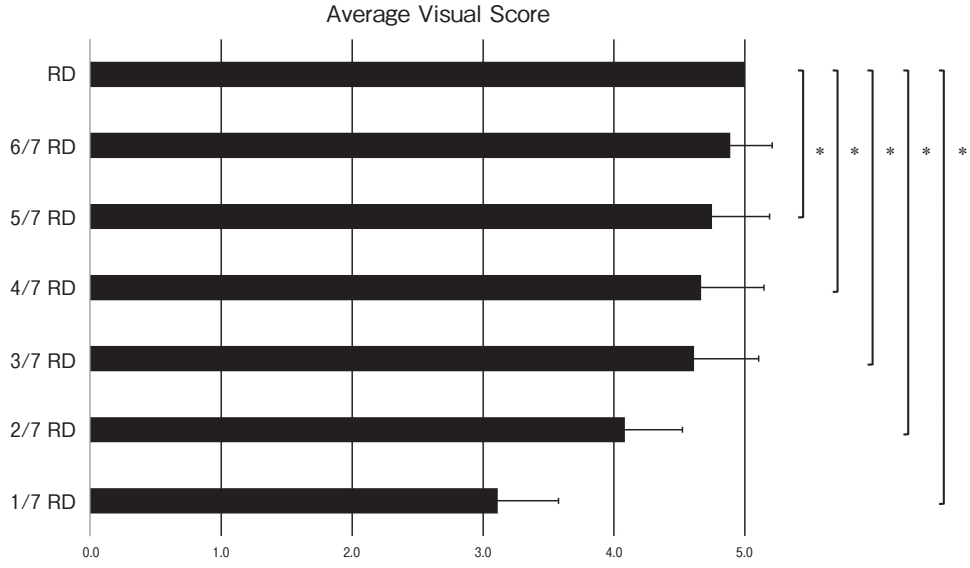

Fig. 3 The average visual scores of the ear ossicles. The average scores of the RD (5.0), six-sevenths of the RD (4.9 ± 0.3), five-sevenths of the RD (4.8 ± 0.4), four-sevenths of the RD (4.7 ± 0.5), three-sevenths of the RD (4.6 ± 0.5), two-sevenths of the RD (4.1 ± 0.4), and one-seventh of the RD (3.1 ± 0.5) are shown. $^{*}p < 0.01$.

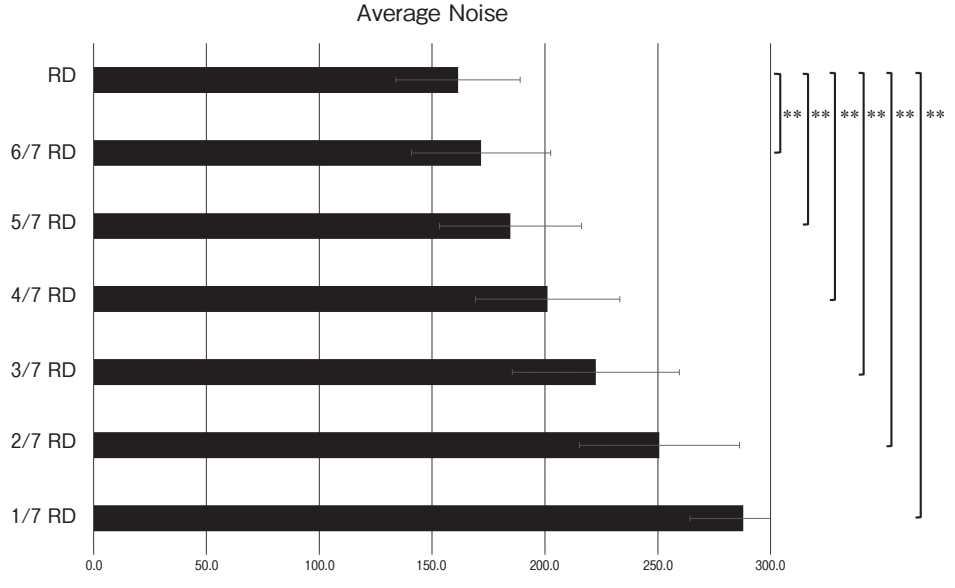

Fig. 4 The average noise of the images of pig ear ossicles. The average noise values for the RD (161.5 ± 27.6), six-sevenths of the RD (171.7 ± 30.8), five-sevenths of the RD (184.7 ± 31.5), four-sevenths of the RD (201.2 ± 32.0), three-sevenths of the RD (222.5 ± 37.0), two-sevenths of the RD (250.7 ± 35.5), and one-seventh of the RD (287.9 ± 23.7) are depicted. $^{**}p < 0.001$.

assessment, only the score of the images at six-sevenths of the RD was not significantly different from those at the RD. Even the mean score of the images at three-sevenths RD was >4.5, suggesting that imaging using a dose as small as half the RD may be clinically acceptable.

Computed tomography is an indispensable diagnostic tool for ear diseases because it excels in depicting changes in the ossicles and soft tissues against background air in the middle ear cavity [8]. However, in CT

scans of this region, certain body parts. such as the temporal bone, have a limited volume (z-axis) and require very high resolution. In examinations using conventional EID-CT, it is challenging to reduce the radiation dose, and there have been reports of imaging protocols that reduce the radiation dose to the lens and techniques to reduce the radiation dose, such as iterative reconstruction methods [9-11].

Hearing loss is often detected during early childhood and may require repeated pre- and postoperative CT examinations to evaluate its cause and/or the hearing status after surgery. Children are more radiosensitive than adults, and the associated potential cancer risk from ionizing radiation makes reducing the radiation dose an important issue [12].

PCD-CT produces high-resolution images with less image noise compared to EID-CT [13]. Its beneficial applications include imaging of the heart, lungs, and bone structures of the wrist, where the exquisite spatial resolution adds clinical value [14,15]. PCD-CT can also be clinically useful for temporal bone CT because of its ability to image small changes in the ear ossicles at high-resolution [1,7]. PCD-CT is thus well suited for evaluating diseases such as ossicular chain dislocation, tympanosclerosis, and cholesteatoma [1].

A few studies have compared PCD-CT and EID-CT in terms of their usefulness in the assessment of bone [15-17]. A comparison of PCD-CT with EID-CT using a human cadaveric wrist showed that PCD-CT provided better delineation of small nondisplaced fractures and changes in bone structure due to fracture and healing than EID-CT, and gave superior visualization of the wrist bone structure even at half the dose [15]. Bette *et al.* [16] and Gruntz *et al.* [17] also demonstrated that the overall image quality and bone assessment were better with PCD-CT despite the decreased contrast noise ratio and increased noise. These previous reports and our present findings are consistent, indicating that diagnostic imaging is feasible even with a reduction from the RD.

Several study limitations bear mention. Pig ear ossicles, not human ear ossicles, were used for the evaluation. However, the pig middle-ear anatomy is highly comparable to that of humans [18], and we thus considered it a suitable model for the middle ear. Despite this limitation, the dose reduction was based on the recommended dose, suggesting the possibility of a significant reduction in the radiation dose from the recommended dose in human ear ossicles (since they are smaller than those in pigs) based on our results. We focused on radiation dose reduction and visual evaluation under imaging conditions used in clinical practice, and future research should include contrast with conventional EID-CT and objective evaluations of the reconstruction kernel and modulation transfer function.

In addition, two raters were involved in this study, and their rate of agreement was unexpectedly high. This was unlikely to be attributable to variation by chance, since the kappa coefficient obtained in this study was 0.6171, but $p < 0.0001$. It is also possible that the two raters systematically made similar judgments. This possibility could make it difficult to generalize the present results.

In conclusion, temporal bone CT images acceptable for use in clinical diagnosis were obtained in pigs even when the radiation dose was reduced to three-sevenths of the recommended dose, a reduction of approximately 50%. This result may serve as one reference for reducing radiation exposure in patients undergoing CT scans.

Availability of data and materials. The data that support the findings of this study are not openly available due to reasons of sensitivity; they are available from the corresponding author upon reasonable request. The data are located in controlled-access data storage at Okayama University Hospital.

References

1. Takahashi Y, Higaki F, Sugaya A, Asano Y, Kojima K, Morimitsu Y, Akagi N, Itoh T, Matsui Y and Hiraki T: Evaluation of the ear ossicles with photon-counting detector CT. Jpn J Radiol (2024) 42: 158–164.
2. Larem A, Abu Rajab Altamimi Z, Aljariri AA, Haidar H, Elsotouhy A, Alsaadi A and Alqahtani A: Reliability of high-resolution CT scan in diagnosis of ossicular tympanosclerosis. Laryngoscope Investig Otolaryngol (2021) 6: 540–548.
3. Nakamura Y, Higaki T, Kondo S, Kawashita I, Takahashi I and Awai K: An introduction to photon-counting detector CT (PCD CT) for radiologists. Jpn J Radiol (2023) 41: 266–282.
4. Esquivel A, Ferrero A, Mileto A, Baffour F, Horst K, Rajiah PS, Inoue A, Leng S, McCollough C and Fletcher JG: Photon-counting detector CT: key points radiologists should know. Korean J Radiol (2022) 23: 854–865.
5. Rajendran K, Petersilka M, Henning A, Shanblatt ER, Schmidt B, Flohr TG, Ferrero A, Baffour F, Diehn FE, Yu L, Rajiah P, Fletcher JG, Leng S and McCollough CH: First clinical photon-counting detector CT system: technical evaluation. Radiology (2022) 303: 130–138.

6. McCollough CH, Rajendran K, Leng S, Yu L, Fletcher JG, Stierstorfer K and Flohr TG: The technical development of photon-counting detector CT. Eur Radiol (2023) 33: 5321–5330.
7. Rajendran K, Voss BA, Zhou W, Tao S, DeLone DR, Lane JI, Weaver JM, Carlson ML, Fletcher JG, McCollough CH and Leng S: Dose reduction for sinus and temporal bone imaging using photon-counting detector CT with an additional tin filter. Invest Radiol (2020) 55: 91–100.
8. Juliano AF, Ginat DT and Moonis G: Imaging review of the temporal bone: part II. Traumatic, postoperative, and noninflammatory nonneoplastic conditions. Radiology (2015) 276: 655–672.
9. Leng S, Diehn FE, Lane JI, Koeller KK, Witte RJ, Carter RE and McCollough CH: Temporal bone CT: improved image quality and potential for decreased radiation dose using an ultra-high-resolution scan mode with an iterative reconstruction algorithm. Am J Neuroradiol (2015) 36: 1599–1603.
10. Niu YT, Mehta D, Zhang ZR, Zhang YX, Liu YF, Kang TL, Xian JF and Wang ZC: Radiation dose reduction in temporal bone CT with iterative reconstruction technique. Am J Neuroradiol (2012) 33: 1020–1026.
11. Niu Y, Wang Z, Liu Y, Liu Z and Yao V: Radiation dose to the lens using different temporal bone CT scanning protocols. Am J Neuroradiol (2010) 31: 226–229.
12. Pearce MS, Salotti JA, Little MP, McHugh K, Lee C, Kim KP, Howe NL, Ronckers CM, Rajaraman P, Sir Craft AW, Parker L and Berrington de González A: Radiation exposure from CT scans in childhood and the subsequent risk of leukemia and brain tumors: a retrospective cohort study. Lancet (2012) 380: 499–505.
13. Pourmorteza A, Symons R, Henning A, Ulzheimer S and Bluemke DA: Dose efficiency of quarter-millimeter photon-counting computed tomography: first-in-human results. Invest Radiol (2018) 53: 365–372.
14. McCollough CH, Rajendran K, Baffour FI, Diehn FE, Ferrero A, Glazebrook KN, Horst KK, Johnson TF, Leng S, Mileto A, Rajiah PS, Schmidt B, Yu L, Flohr TG and Fletcher JG: Clinical applications of photon counting detector CT. Eur Radiol (2023) 33: 5309–5320.
15. Booij R, Kämmerling NF, Oei EHG, Persson A and Tesselaar E: Assessment of visibility of bone structures in the wrist using normal and half of the radiation dose with photon-counting detector CT. Eur J Radiol (2023) 159: 110662.
16. Bette SJ, Braun FM, Haerting M, Decker JA, Luitjens JH, Scheurig-Muenkler C, Kroencke TJ and Schwarz F: Visualization of bone details using a novel photon-counting dual-source CT scanner compared with energy-integrating CT. Eur Radiol (2022) 32: 2930–2936.
17. Grunz JP, Huflage H, Heidenreich JF, Ergün S, Petersilka M, Allmendinger T, Bley TA and Petritsch B: Image quality assessment for clinical cadmium telluride-based photon-counting computed tomography detector in cadaveric wrist imaging. Invest Radiol (2021) 56: 785–790.
18. Hoffstetter M, Lugauer F, Kundu S, Wacker S, Perea-Saveedra H, Lenarz T, Hoffstetter P, Schreyer AG and Wintermantel E: Middle ear of human and pig: a comparison of structures and mechanics. Biomed Tech (Berl) (2011) 56: 159–165.